Eur. Phys. J. E **1**, 189–194 (2000)

THE EUROPEAN PHYSICAL JOURNAL E

EDP Sciences

Experimental model of cracking induced by drying shrinkage

H. Colina[1] and S. Roux[2,a]

[1] Laboratoire Environnement, Gomcanique et Ouvrages, B.P. 40, 54501 Vandœuvre-lès-Nancy Cedex, France
and
Universidad Nacional de Salta Buenos Aires 177, 4400 Salta, Argentina
[2] Laboratoire "Surface du Verre et Interfaces"[b], B.P. 135, 93303 Aubervilliers Cedex, France

Received 19 April 1999

Abstract. Drying induced shrinkage in materials may yield the formation of surface crack patterns. We report on various experimental observations of the geometry of the crack array and the kinetics of crack formation on a model system consisting of a layer of a paste made of clay, sand, and water deposited on a rigid substrate. We investigate in detail the influence of the layer geometry (size and thickness).

PACS. 92.40.Lg Soil moisture – 46.50.+a Fracture mechanics, fatigue and cracks – 46.65.+g Random phenomena and media

1 Introduction

Water which is not consumed during the manufacturing and later hardening of some materials (such as concrete, cement, plaster, ...) leads upon drying to a shrinkage of the material. Drying from a free surface gives rise to an inhomogeneous shrinkage which in turn produces stresses which may lead to cracking, when they exceed the material strength.

It is only in concrete pieces of a small size that shrinkage can be uniform enough to prevent crack formation [1]. In general, surface elimination of water gives rise to tensile stresses in the skin of the material which are partly released by the formation of surface cracks. The latter form a characteristic polygonal pattern in brittle homogeneous materials (*e.g.* cement), and a more complex dense array of branched cracks in more heterogeneous structures (standard concrete and mortar). Indeed heterogeneities will favour [2–4] the nucleation of stable micro cracks which progressively shields the stress, and gives rise to a "controlled" development of cracking. In contrast, for homogeneous materials, the nucleation of cracks is the limiting process. As soon as they are initiated, they tend to propagate extremely fast along the surface in a more or less straight manner until they are stopped by other preexisting cracks. The latter scenario gives a mosaic where at least past of the history of crack formation can be read from the final pattern.

It is crucial to understand the pattern formation of surface cracks in concrete structures, in particular for their ageing properties. Surface cracks are easy paths for chemical species which may react with the material or reinforcements. Thus estimating the depth and opening of cracks is essential. The latter are however difficult to measure directly. It is thus of interest to try to relate these properties to the surface crack pattern, which is much more easily accessible.

Motivated by the previous arguments, we carried out experiments in concrete on samples of typical size 1 m^3, in order to obtain crack networks that can be macroscopically observed and which are independent of the sample size [5–7]. However, the duration of the cracking process which increases dramatically with the system scale [8,9] did not allow us to appreciate final patterns because an evolution was still noticeable when the experiment was stopped after more than one year [6]. Thus, it was not possible to perform parametrical or statistical studies on test pieces of such sizes. This led us to develop and study systematically a model system where the time evolution is more convenient. However, the parallel with concrete should be considered critically, since dessication shrinkage is only one among many other complex phenomena taking place during concrete setting. In particular, "weathering" may affect considerably the crack opening close to the free surface, thereby limiting any meaningful comparison with the much simpler clay/sand system we study in the present paper.

Skjeltorp [10] has reported on the experimental study of such a model system consisting of a monolayer of equal-size spherical particles laid on a rigid substrate. This nice, inspiring experiment is extremely sensitive to the detail of the microstructure of the layer. The spheres naturally form a regular "crystal", and thus the cracks follow the principal axes of this array. It is difficult with this system to change either the disorder or the geometry of the

[a] e-mail: stephane.roux@sgr.saint-gobain.com
[b] Unit mixte de Recherche CNRS/Saint-Gobain

(a) (b) (c) (d)

Fig. 1. Crack arrays obtained at the end of the drying process in four samples with an initial 160×160 mm^2 square drying surface, and with initial thickness: (a) $e = 16$ mm, (b) 10 mm, (c) 4 mm and (d) 2 mm.

sample. Meakin [11] has proposed a numerical modelling of this phenomenon. More recently, Groisman and Kaplan [12] have carried out experiments with coffee-water mixture, studying the final pattern of cracks with special interest in the cracking network and in the joining angles between cracks. Field experimental observation has been also made by Konrad and Ayad [13] to document the formation of shrinkage cracks in an intact and weathered sensitive marine clay. Interesting results are reported and a mechanism of crack propagation is suggested. These data were used by Ayad, Konrad and Souli [14] to asses the performance of a numerical model enabling the prediction of depth and spacing of cracks. However, these experiences are strongly dependent on the soil history and location.

2 The experimental model

The material we chose for our experiment is clay. It indeed gave rise to crack patterns in a reasonable time (from hours to days depending on the thickness) reproducibly. Clay is also a very workable material and it does not display significatively endogenous phenomena. These qualities make clay better than other materials for our model. It allows for easy variations in the initial size and thickness. And finally it is possible to adjust the homogeneity of the material although this point was not used in the present study. Clay was mixed with sand in order to promote the formation of small cracks. Without sand a qualitatively similar phenomenology was observed but with a much less dense array of cracks.

After a number of different trials, we selected the following system: two series of samples were made with a superfine clay composed of illite, kaolinite and smectite, and 21% in volume of fine sand (typical granulometry 0.15 mm). The mix was then supersaturated with water to obtain a paste, free of air bubbles which could easily be poured. The sand granulometry was chosen small enough to avoid significant sedimentation in the mold. The tixotropy of the clay was also helpful to prevent or limit sedimentation. Samples had a parallelipedic shape with a square face $L \times L$ exposed to drying and initial thickness e. Drying was monitored by controlled hot air circulation (29 °C and 32.5% hygrometry). The sample size was varied to study size effects. The first series had a variable initial thickness, e, with a constant drying surface, L, fixed, while the second had a fixed thickness and a variable drying surface.

2.1 Test development

For the first series, the drying surface was initially a 160×160 mm^2 square. The initial thickness e was 16, 10, 4 and 2 mm. Figure 1 shows the final geometry of crack patterns obtained for this series, and shows that the thickness is a determining parameter for controlling the crack density.

The second series was chosen with a variable drying surface. The thickness was kept constant and equal to that giving rise to the most interesting and meaningful crack pattern of the previous series, namely $e = 2$ mm. Indeed for thicker samples, the distance between cracks is not very small compared to the sample lateral size. The selected surfaces were squares of initial size $L = 20$, 80 and 40 mm

This second series was not anticipated to provide any appreciable difference in the crack patterns. However the mean crack spacing was observed to increase for the two smaller samples.

3 Analysis of the experimental results

3.1 Geometrical properties

The cracks can be characterised by their spacing, their opening and their depth. The spacing is the easiest parameter to determine experimentally. The depth can be safely considered as equal to the entire layer thickness in all the studied samples. The crack opening can be estimated indirectly if the shrinkage of the material is known. To estimate it, we measured the variation in sample size and thickness after drying. Note that the lateral size reduction is only apparent since it is estimated from the end to end size and includes also the crack density and opening. It was possible to measure experimentally the crack opening only for thicknesses larger or equal to 4 mm.

We have verified [6] the expected fact that the thicker the sample, the larger the crack opening.

During the entire time evolution of the experiences, we periodically took photographs of the drying surfaces. These pictures were digitised and recorded. We used standard image processing techniques to threshold the grey pictures to black and white, which after skeletonization, gave a fairly accurate description of the crack array. The procedure used for estimating the crack spacing is the following [6,7]: a set of lines was drawn with different orientations and counted the number of intersections between the line and the cracks, inside a domain which excluded the edges of the samples. From these intersections, we deduced the average length of segments which we identify with the mean crack spacing ℓ. Note that this measurement does not require the cracks to be connected. This crack spacing can only be compared to the typical "fragment" size if they have a regular convex shape. When no more evolution of the crack pattern could be detected, we considered the evolution as terminated. We call $\ell_{\rm f}$ the final crack spacing.

We introduced the aspect ratio of the sample defined to be $\alpha = L/e$. We also define φ, the dimensionless crack spacing, as $\varphi = \ell/e$. Analysing the collected data [6], we find that the final relative crack spacing could be reasonably described by the following exponential form:

$$\varphi_{\rm f} = A + K\exp(-c\alpha) \tag{1}$$

where A, K and c are dimensionless constants with the following values:

$$\begin{aligned} A &= 2.9 \pm 0.2, \\ K &= 3.9 \pm 0.3, \\ c &= 0.054 \pm 0.004. \end{aligned} \tag{2}$$

Equation (1) indicates that for a very large system size, the final crack spacing tends to a constant, so that the distance between cracks is simply proportional to the sample thickness. Such a result has already been observed in other systems [12]. However, the correction observed for small system sizes – small or thick samples having a larger spacing – is original.

In Figure 2 we can see a reasonable agreement between the experimental data and the curve described by equation (1). In the figure, we have indicated the constant A, which gives the asymptotic value of $\varphi_{\rm f}$ for large α. Since it is impossible to have a crack spacing l larger than the initial length L, this figure gives a lower limit of α, $\alpha_{\rm min}$, such that no macroscopic cracking can be observed. This value is obtained by equating $\varphi_{\rm f}(\alpha_{\rm min}) = \alpha_{\rm min}$. This last parameter defines an objectivity threshold $\alpha_{\rm min} \approx 5.8$ as shown in Figure 2.

The minimum value has been confirmed by the following experimental test: some samples were produced with $\alpha < \alpha_{\rm min}$, and none of them displayed inner cracks when dried. Some cracks were initiated close to edges (and in particular in the corners) but they never propagate inside the sample (see Fig. 1). This fact has been verified even for cubic samples, $\alpha = 1$, which have dried through only one face.

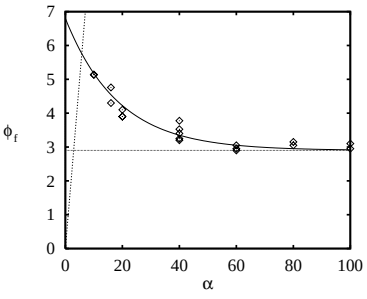

Fig. 2. Average crack spacing relative to the sample thickness, $\varphi_{\rm f}$, as a function of the aspect ratio of the sample, α. The asymptotic value is shown as a dotted line.

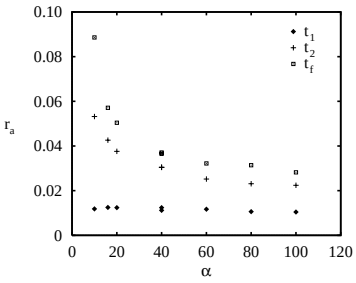

Fig. 3. Apparent shrinkage $r_{\rm a}$ distribution as a function of the initial aspect ratio a at three characteristic times (t_1, t_2 and $t_{\rm f}$).

To estimate the shrinkage, we have computed the apparent surface shrinkage at different characteristic times, t: the beginning of the cracking, t_1, the end of the crack progression, t_2, and the end of the drying, $t_{\rm f}$. We will come back below in detail to these times. We have measured the average side lengths at anyone of these relative times on the images that we have taken during the tests. Then we have calculated the apparent shrinkage, $r_{\rm a}$:

$$r_{\rm a} = \frac{L - L(t)}{L} \tag{3}$$

where $L(t)$ is the length of the sample at time t. Figure 3 shows $r_{\rm a}$ as a function of α for the three times t_1, t_2 and $t_{\rm f}$.

Before t_1, or precisely until the apparition of the first crack, the shrinkage is faithfully measured. Thus it should be independent of the system size (assuming drying is homogeneous in the thickness and that no size effect affects the material strength). This independence is indeed confirmed from the data displayed in Figure 3, which is well peaked on a constant value (≈ 0.012). This value corresponds to the shrinkage such that the tensile stress in the layer reaches the strength of the medium.

When cracks appear, the data begin to be scattered. The real shrinkage is underestimated by an amount of the order of w/ℓ, where w is the mean crack opening. As simultaneously, the real and the apparent shrinkage, ℓ and w evolve with time, and are not measured, we cannot directly use this relation to determine w from the previous quantities. However, this represents a potential way to measure w indirectly.

3.2 The evolution of the physical characteristics

This section is devoted to the study of the kinetics of drying. Recording the weight as a function of time, we could detect three distinct stages for the drying. In Figure 4 we

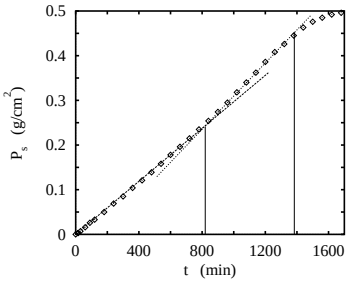

Fig. 4. Time evolution of the loss of weight P_s per unit drying area. Two linear fits are indicated as dotted lines. The cross-over times t_1 and t_2 as shown are vertical thin lines.

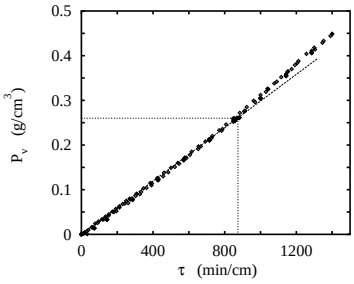

Fig. 5. Loss of weight per unit volume P_v as a function of a scaled time $\tau = t/e$, *i.e.* time divided by the initial thickness, for all sample geometries. The initial regime is fitted by a linear law shown as a dashed line. This fit extends up to $t \approx 870$ s after which the drying rate seems to increase.

show the loss of weight (*i.e.* the decrease in water content) per unit drying area, in a particular sample representative of all other records.

Kayyal [15] has reported similar results for the drying of clay marl specimens but with only one constant rate period for moisture loss. He assumes that all shrinkage effects take place in this stage despite no shrinkage crack being observed in the samples, maybe owing to their size ($\alpha \approx 0.5$). In our observations, the first period, which is generally the longest one, concerns the sample with no cracks. It corresponds to a constant water flux. Drying is not dependent on the water content, indicating that the kinetics is most probably limited by the evaporation along the free surface, the latter being controlled by the incoming flux of hot/dry air. In a second (shorter) stage, the water flux is still constant but markedly higher than in the first regime. Visual inspection shows that cracks are being formed in this period. This may suggest that the crack surfaces allow for a larger surface exchange, thus increasing mass transfer.

However, the relative increase of exchange surface due to this process seems too small to account for such a change in water flux. One may also consider the possibility that the liquid/vapour interface begins to invade the clay matrix, again increasing the surface of exchange, in much more significant proportion. This implies that capillary effects will induce a depression in the free water contained in the material. This depression has to be partly counterbalanced by a compression of the solid skeleton (clay particles and flocs and sand), the unbalanced depression stress gives rise to a total tensile stress in the thickness which is maintained in equilibrium by the friction on the substrate. This skeleton is however expected to be rather weak initially, and thus under isotropic compression it is likely to compress plastically, decreasing its pore volume. This plastic compression of the solid matrix can be thought to take place in a quasi-perfect plastic solid so that the position of the liquid/vapour water interface remains very close to the free surface. Local "break-through" of the interface in the thickness are then naturally identified with the crack nucleation.

Finally in a third period, the drying ceases progressively. In the spirit of the previous explanation, we may assume that the solid matrix compression has reached a sufficient level of hardening so that it can sustain the depression of water corresponding to the pore invasion. In this case, diffusion of water in the clay matrix is the limiting process, and drying becomes much slower than the previous stages.

Considering the pictures of the surface recorded simultaneously show that most cracking happens in the second period. This confirms the picture that the first stage corresponds to a supersaturated medium, (actually closer to a concentrated colloidal suspension with a finite yield threshold than to a solid material) and drying has only a very mild mechanical impact. The third period corresponds to a rather moderate loss of water which does not induce a large shrinkage, and thus does not produce cracks.

These observations lead us to introduce three characteristic times:

(i) t_1, the beginning of cracking, which is directly proportional to the sample thickness. The loss of weight per unit volume is the same for all samples;

(ii) t_2, the end of cracking, which is also directly proportional to the sample thickness. However, in contrast to the previous time, the loss of weight is not the same for all samples but changes with the lateral size L. This time t_2, appears to increase with L;

(iii) t_f, the end of drying. This time is not accurately defined since drying ceases very slowly. However, we refer to times such that no evolution is perceivable. Typically, for quantities labelled by t_f, we performed measurements a few days after no evolution could be detected neither on the water content (weight), nor on the crack pattern.

From the above reported observations, we deduce that most of the interesting data for all sample geometries can be obtained from a plot of the loss of weight per unit volume as a function of the time divided by the thickness $\tau = t/e$. In these scaled variables, all data points fall onto the same "master" curve as shown in Figure 5. In particular, the onset of cracking, t_1/e is the same point for all samples. At this point, the water loss is about 0.260 g/cm^3. The end of the crack evolution t_2 however does not exactly collapse to the same point, as discussed above. An approximate method for determining t_2 from a reference case has been discussed in reference [6].

3.3 Morphology of the crack array

The final part of our analyses deals with the statistical analysis of the crack pattern. A lot of emphasis was put recently on the determination of long range correlation in crack geometry or in damage fields. In particular, self-similarity [16] was reported in some experimental observations and various statistical models [2,3,17–19] have been considered to account for such properties.

To perform this analysis, we have applied standard techniques (see *e.g.* [16]) based on the digitised images taken during the experiments. Two different kinds of pictures were taken, video recording, and traditional photographs. The latter have proved to be much less noisy and safer to analyse. Once digitised, the images were subjected to standard image analysis techniques to extract the crack array. The correlation analysis was then applied using different sets of image processing parameters and was shown to be insensitive to the precise choice of the former, in a range of acceptable values (as judged from visual inspection of the original and binarised images). In some cases, the crack patterns are greatly modified close to the edges of the system because of different drying conditions. In those cases, the images used in the processing were selected in the homogeneous part of the sample to avoid spurious bias.

We have selected the largest connected cluster of cracks. The connectivity is defined on the binarised version of the images after processing. Thus connectivity is easily and unambiguously defined, but one may suspect that it is very sensitive to the various image processing steps. The processing was indeed selected in order to minimize the sensitivity of the cluster morphology on the processing. Although some variability could still be observed depending on the precise series of operations when the entire cluster is considered, we checked carefully that the following pair correlation data were robust with respect to the choice of processing steps which could be considered as reliable from a simple visual inspection.

We computed the number of pixel pairs $c(r)$ at a distance r from each other which both belonged to the cluster. The cumulative sum

$$C(r) = \int_0^r c(r')\mathrm{d}r' \tag{4}$$

was then estimated. For self-similar sets, $C(r)$ is expected to scale as

$$C(r) \propto r^D \tag{5}$$

where D is the fractal dimension.

In Figure 6 we show the obtained results for one of the samples. The log-log plot of $C(r)$ shows that below a characteristic scale, r^*, $C(r)$ is proportional to r showing that the cracks are essentially one-dimensional. We checked that r^* was not related to the image processing technique and the same value was obtained using different magnifications. The scale r^* can be interpreted as the size over which stresses are screened, so that the presence of a crack prevents the apparition of a new one. With this interpretation in mind, it appears sensible to expect a simple proportionality between r^* and e.

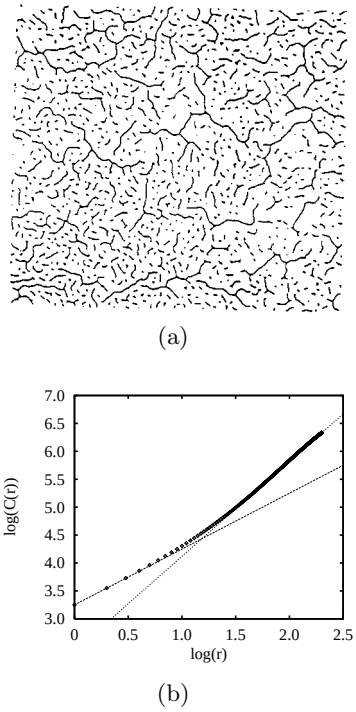

Fig. 6. (a) Binary skeleton and (b) log-log plot for a sample of thickness $e = 2$ mm, and size $L = 200$ mm, after 390 min of drying. Above the scale r^*, we estimate $D \approx 1.7$.

Above r^*, $C(r)$ has a much larger slope which is however definitely smaller than two. This indicates that the cluster develops a fractal structure above r^*, with a fractal dimension measured to be about $D \approx 1.7$. We note that this property is specific to crack clusters, and does not apply to the entire crack array, which clearly is expected to display a dimension equal to 2, that of the embedding space.

It would have been difficult to argue for the value of such a fractal dimension if we had one single example of such results. However, the consistency of the determination of this dimension among all of the samples in which the correlation length is much smaller than the system size gives us some confidence in the result, and on the robustness of the image processing steps. Moreover, a slow cross-over from $D = 1$ to $D = 2$ giving rise to apparent exponent intermediate between these cases seems unlikely, in particular if we compare the data to those corresponding to all cracks (and not only the largest connected cluster), where indeed such a cross-over is observed.

Similar estimates of the fractal dimension were obtained on all processed images, for a sample thickness less than 10 mm. Above this thickness, the cracks appear to be simple straight cracks, and the microscopic scale r^* becomes of the order of the system size L, so that extremely large samples would have been needed to observe the fractal regime. The cross-over scale r^* increases with the thickness e, but we do not have enough data to quantify precisely this variation.

We also note that a similar analysis on concrete samples of 1 m size (mentioned in the introduction) produces

a comparable result $D \approx 1.7$ [6,7]. However, we do not have any satisfactory model to account for this result. Most simple models rather suggest a fractal dimension equal to two, above a screening length, since the origin of cracking is due to the shrinkage process which is taking place homogeneously in the medium.

4 Discussion

In this section, we would like to suggest possible extensions of our results to more general cases.

We first note a strong analogy between the shrinkage problem and an original mechanical test devised to identify at least a softening damage behaviour. The latter generally leads to localisation of the strain so that even for a homogeneously stressed sample the load-displacement characteristic cannot give faithful information on the constitutive law of the material. In order to prevent localisation, it was proposed [20] to glue the studied sample to an elastic medium (with the same initial elastic modulus) loaded in parallel. The presence of a crack could then only affect a finite portion of the studied sample, outside load is transferred back to the sample from the elastic piece. We note that the uniformly strained elastic medium plays the same role as the rigid substrate in our problem. This analogy suggests that the set-up should be characterised by an effective screening length, ξ, depending on the precise geometry of the two materials, so that the resulting behaviour law extracted from the test results should still be non-intrinsic, depending on ξ but no longer on the sample size L, provided $L \gg \xi$.

We have considered a model system where essentially all properties were homogeneous in the thickness. However, for massive structures, typical cases will be that the water-content depends on the depth below the surface. For a simple diffusion the water content profile is a rapidly decreasing function (for a thick medium) with a characteristic scale h equal to

$$h = \sqrt{2D_H t} \tag{6}$$

where D_H is a diffusion coefficient and t is the time. We could however think of transposing the results obtained above to such a case, replacing e by h. With such a scenario, we expect to see shortly after the beginning of drying the formation of a dense network of shallow cracks. Then, as time progresses, cracks should compete with a selection such that the spacing between active cracks should scale as h. Thus the network of cracks is expected to evolve toward less and less dense crack array but with deeper cracks.

This scenario is actually very similar to one observed in the opposite case of swelling. Tanaka [21] has studied the morphology of the surface of a gel swelling from the diffusion of salt from its surface. The swelling lead to a buckling of the surface with a characteristic length equal to a diffusion length.

5 Conclusion

From the study of our model system, we have clarified the importance of size effects in surface cracking due to drying shrinkage. We have seen that the mean crack spacing is essentially controlled by the thickness of the sample but can be significantly increased for small samples. A quantitative analysis suggested the existence of a minimal aspect ratio, below which no (macroscopical) crack develops in the material. The kinetics of drying has shown the existence of three distinct phases, with only the second one producing cracks. The onset of crack initiation could be formulated in a quantitative size-independent criterion, in terms of water content, or alternatively for the ratio of time over sample thickness. The end of the cracking process however did not scale in a similar way.

Finally, analysing the morphology of large crack clusters, we showed the existence of a characteristic size (depending on the thickness) over which cracks are essentially linear objects (and thus below which stress screening is effective). Above this scale, the cracks tend to form a self-similar structure of dimension $D \approx 1.7$.

References

1. P. Acker, rapport de recherche LPC, n° 152 (1988).
2. See, *e.g.*, *Statistical Models for the Fracture of Disordered Media*, edited by H.J. Herrmannx, S. Roux (North-Holland, Amsterdam, 1990).
3. See, *e.g.*, *Disorder and Fracture*, edited by J.-C. Charmet, S. Roux, E. Guyon (Plenum, New York, 1990).
4. H. Colina, L. de Arcangelis, S. Roux, Phys. Rev. B **48**, 3666 (1993).
5. L. Oger (unpublished, 1988).
6. H. Colina, Ph.D. thesis, École Nationale des Ponts et Chausses, Paris, France, 1992.
7. H. Colina, in *Proceedings of the 1st Sympotium in Structures, Geotechnic and Construction Materials*, Santa Clara, Cuba, 1994.
8. L. Granger, J.-M. Torrenti, P. Acker, Mater. Struct. **30**, 96 (1997).
9. H. Colina, P. Acker, in *Proceedings of the Congress in Valorization of Public Works and Building Research and its Associated Industries*, Rabat, Maroc, 1998.
10. A.T. Skjeltorp, in *Time Dependent Effects in Disorder Materials*, edited by R. Pynn, T. Riste (Plenum, NewYork, 1987).
11. P. Meakin, Thin Solid Film **151**, 165 (1987).
12. A. Groisman, E. Kaplan, Europhys. Lett. **25**, 415 (1994).
13. J.-M. Konrad, R. Ayad, Can. Geotech. J. **34**, 929 (1997).
14. R. Ayad, J.-M. Konrad, M. Soulie, Can. Geotech. J. **34**, 943 (1997).
15. M. Kayyal, in *Unsaturated Soils*, edited by Alonso and Delage (Balkema, Rotterdam, 1995).
16. J. Feder, *Fractals* (Plenum, New York, 1988).
17. E. Louis, F. Guinea, Europhys. Lett. **3**, 871 (1987).
18. D. Sornette, J. Phys. France **50**, 745 (1988) .
19. E.L. Hinrichsen, A. Hansen, S. Roux, Europhys. Lett. **8**, 1 (1989).
20. J. Mazars, Y. Berthaud, S. Ramtani, Eng. Fracture Mech. **35**, 629 (1990)
21. T. Tanaka, in *Statistical Research on Fatigue and Fracture*, edited by T. Tanaka, S. Nishijima, M. Ichikawa (Elsevier, London, 1987).